FLM: Wiring Controls, Context and Local Credit

A sixty-run diagnostic study with mixed topology effects

Kuber Mehta
flm.kuber.studio

12 September 2026 — status-updated working note

Abstract

Does measured wiring help the computation performed by an artificial fly-wired network? We compare five learning rules on measured and constrained-randomized graphs in two delayed-choice tasks. Sixty fixed-budget runs share initial parameters and sensory streams within each task and each of three seed pairs. At the final 48-frame cue probe, full backpropagation through time (BPTT) averages 100.00% with measured wiring and 66.67% with randomized wiring. For the harder delayed-context task at delay eight, the ordering reverses: 63.02% versus 76.04%. Gradient probes quantify departures of local eligibility estimates from exact temporal credit. These mixed results establish no general anatomical or local-learning advantage. This is a small artificial-task study. The separate, now-completed WikiText topology report finds no measured-wiring advantage for its selected language subset; a distinct 128-fit selection follow-up has no held-out result yet.

1 The comparison that is needed

FLM uses measured neural edges as a fixed prior for a trainable recurrent rate network. Successful task learning alone does not show that measured wiring is useful: the same machinery may work as well on an appropriate random graph. Connectome-constrained visual-system evidence concerns different predictions [1]. A recent flyvis preprint illustrates how initialization and null-model choices can weaken an apparent topology effect [2]. Neither source establishes an FLM language advantage.

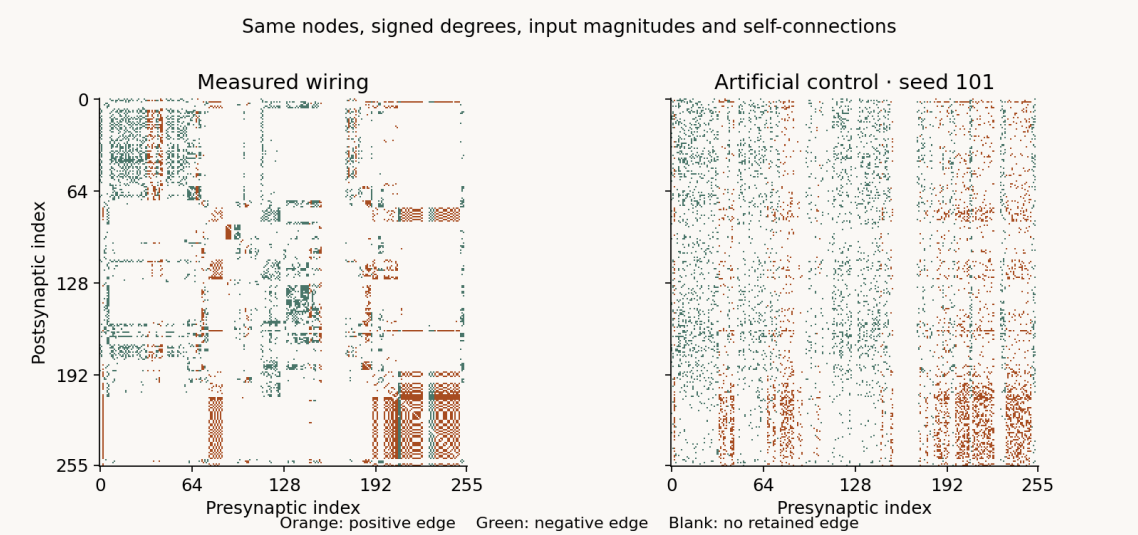

Figure 1: Measured 256-neuron subset and one artificial control, in the same node order. Rows are postsynaptic and columns presynaptic. The control preserves degrees, input signs and magnitudes, and original self edges. New edges are artificial; their transferred contact values are not measured new synapses.

2 Matched graph and learning machinery

The measured graph retains 256 central intrinsic MaleCNS neuron identities, 6,678 directed edges and 32 output pools [3]. It is a different subset from FLM's 1,024-neuron language core. The four sensory inputs and two-action readout are engineered, not biological sensory or descending pathways. All models allocate 8,729 parameters.

Each null begins from the measured graph. A double-edge swap $(i,j),(k,l) \mapsto (i,l),(k,j)$ exchanges presynaptic endpoints only when sources j,l have the same assumed neurotransmitter sign. Reject duplicates, new self edges and unchanged proposals. Preserve every original self edge at its weight; keep all other array slots except the source index unchanged. Each chain accepts ten swaps per edge. This extends a degree-preserving null construction [4] with explicit sign and self-edge constraints.

Thus every neuron's directed in/out degree, target-wise signed incoming weight/contact multiset, node order, coordinates and pool membership match. Outgoing weighted strength, distance, reciprocity and higher motifs need not match. The three nulls retain approximately 23% of original edges. Reciprocal off-diagonal edges fall from 67.96% to 14.74–15.31%. Finite chains do not establish uniform sampling or adequate mixing over all allowed graphs.

The normalized rate recurrence is

$$W_{ij} = \frac{b_{ij}\exp(\theta_{ij})}{\sum_k |b_{ik}\exp(\theta_{ik})|}, \quad z_t = \tanh(Ax_t + b + gWh_{t-1}), \tag{1}$$

$$h_t = (1-\alpha)\odot h_{t-1} + \alpha \odot z_t, \qquad s_t = (1-\beta)\odot s_{t-1} + \beta \odot h_t. \tag{2}$$

Signs of b are fixed; edge logits are bounded to $[-3,3]$. Sigmoids bound $\alpha \in (.05,.95)$, $\beta \in (.002,.100)$ and $g \in (.05,3)$. Pooled fast and slow states pass through LayerNorm and a binary readout.

Five rules use SGD at .03, batch eight, clipping at one, and no momentum or weight decay: full BPTT; fixed-core readout learning (258 effective trainable parameters); supervised forward eligibility; the same approximation with trace history cleared each frame; and reward-modulated eligibility. The forward rules retain direct temporal derivatives but omit indirect temporal routes through other neurons. Instantaneous readout derivatives supply the learning signal. The normalized-edge direct derivative includes $\partial(Wh)_i/\partial\theta_{ij} = W_{ij}h_j - |W_{ij}|(Wh)_i$. Eligibility is motivated by prior work [5], not a new property unique to fly wiring. This rate-network approximation is not a spiking e-prop reproduction.

3 Tasks, phases and experimental units

The cue task has two cue frames, a sampled delay $D \in \{4,\dots,12\}$ and one query frame. The context task adds two later context frames and another delay: $T = 2D + 5$. The answer is cue XOR context. Gaussian distractor input (SD .2) occupies another channel throughout. Batches balance the binary cues or all four cue/context combinations. States reset each episode; weights persist.

All runs train the original rule for updates 1–300, its inverse for 301–600, then the original for 601–900: 7,200 episodes. No phase flag is supplied. Model seeds 17/29/41 are paired with null seeds 101/103/107. The design is two tasks × two topologies × five rules × three seed pairs. Graph and initialization variation are *not* independently crossed here. The 15 measured-cue conditions reproduce the earlier trained tensors and sample-stream hashes exactly; they are bridges, not extra replications.

4 Results: topology effects change with the task

Fixed panels contain 256 balanced episodes at delays 4, 8, 12, 24 and 48, measured initially and every 100 updates. They are reused diagnostics, not untouched test data or checkpoint-selection criteria. Every run finishes at 900; no favorable seed or checkpoint is selected. Equal episodes across tasks do not mean equal numbers of sensory frames or equal computation.

Table 1: Final accuracy (%), three-seed means. These two declared panels show a change in ordering; all 3,000 seed-level observations remain available.

	Cue, delay 48		Context, delay 8	
Learning rule	Measured	Rewired	Measured	Rewired
BPTT	100.00	66.67	63.02	76.04
Fixed core	86.46	55.73	63.15	44.53
Eligibility	83.33	50.00	53.52	57.03
No trace history	50.00	66.93	57.68	55.34
Reward + eligibility	50.00	50.00	66.67	50.00

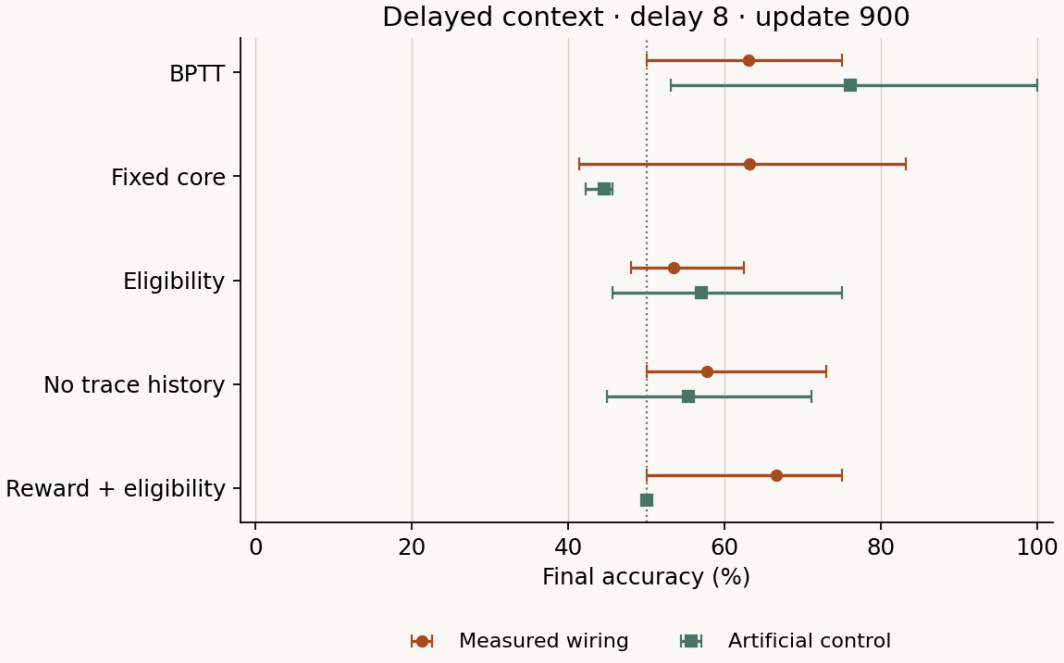

Figure 2: Final context accuracy at delay eight. Markers are means; bars span the observed three-seed range, not a confidence interval. Chance is 50%. Wide ranges preclude a robust ordering based on the mean alone.

The cue task gives measured wiring an advantage for some long-delay conditions, including BPTT, fixed-core and supervised eligibility. That observation does not generalize to the context task. BPTT's measured-minus-null contrast at delay eight averages −13.02 percentage points, with paired seed differences from −50.00 to +10.94. The measured fixed-core mean instead exceeds its null mean by 18.62 points in that panel, again with a seed-dependent sign.

Supervised eligibility does not consistently outperform its no-history or fixed-core alternatives. Most final context conditions approach chance at delay 48; measured fixed-core accuracy averages 57.55%. Reward eligibility's binary correctness feedback also reveals the alternative action's correctness, so this assay does not establish learning from strictly less target information. The complete delays, phases, probabilities and per-seed losses are published.

5 How far is local credit from the exact gradient?

At updates 0, 300, 600 and 900, fixed eight-episode delay-eight probes compare the exact supervised core gradient g with an approximate gradient $\hat{g}$. Copied float64 models ensure that diagnostics never update trained weights or RNG state. The archive reports cosine $g^\top \hat{g}/(\|g\|\|\hat{g}\|)$, relative L2 error, norms and sign agreement for all six core parameter groups and their concatenation. Undefined ratios remain explicit.

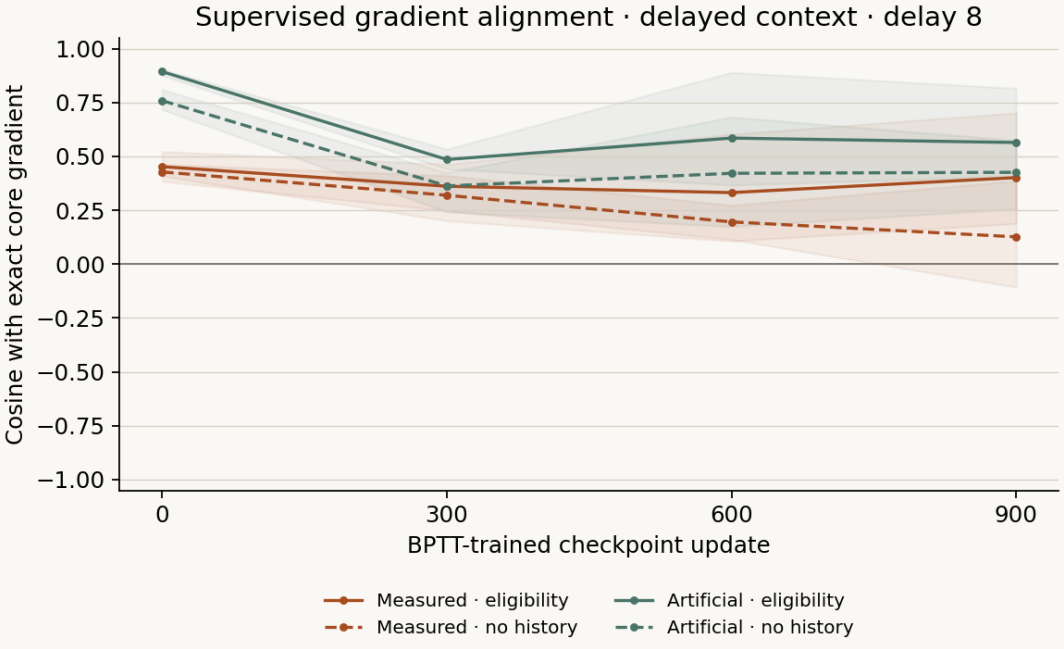

Figure 3: Context task, BPTT-trained checkpoints. Exact-versus-approximate core gradient cosine; lines are seed means and shading their range. This is a supervised derivative diagnostic, including when separately inspecting reward-trained networks. It is not a reward-gradient verification.

Local credit is not exact BPTT and its alignment depends on graph and training state. Better cosine is not sufficient to predict better learning: magnitude, optimization trajectories and the task also matter. Reward-driven models are evaluated with the same supervised probe for comparability, not by equating cross-entropy with their training objective.

6 Limits, language follow-up and reproducibility

There is no general anatomical advantage established by these diagnostics. Only one small subset, three paired seeds, two artificial tasks and one fixed learning budget were tested. Random controls retain substantial anatomical information. Repeated probes are not independent samples, and seed ranges are not uncertainty intervals for populations of graphs or tasks. The body replay study is separate; these results imply neither animal learning nor learned gait.

The language follow-up uses three 1,024-neuron null graphs *crossed* with training seeds 42/43, plus two measured-graph models retrained without slow state, under the original WikiText budget. All eight new runs and ten checkpoint selections completed before new-control test scoring. The completed report finds no measured-wiring advantage in that subset and setup; retaining slow state helps against retrained no-slow controls. These results are reported separately in the main FLM paper. The active 128-fit selection study is a distinct follow-up, with validation and held-out results pending. The original main-language test scores were already inspected, so the extension is exploratory.

The repository describes graph, reference-run and environment prerequisites. Reproduce training and then verify the records with:

```
python -m flm.wiring_study
python -m flm.wiring_report
```

The website provides the declared protocol, graph identities, every retained prediction, CSVs and a 71-entry archive. Tables here are generated from the verified complete records.

References

[1] Janne K. Lappalainen et al. Connectome-constrained networks predict neural activity across the fly visual system. *Nature*, 2024. https://doi.org/10.1038/s41586-024-07939-3.

[2] Nalin Dhiman. Topological sensitivity in connectome-constrained neural networks. https://arxiv.org/abs/2604.04033v1, 2026. Preprint.

[3] Janelia Research Campus. MaleCNS connectome release and downloads. https://male-cns.janelia.org/download/, 2026.

[4] Sergei Maslov and Kim Sneppen. Specificity and stability in topology of protein networks. *Science*, 296:910–913, 2002. https://doi.org/10.1126/science.1065103.

[5] Guillaume Bellec et al. A solution to the learning dilemma for recurrent networks of spiking neurons. *Nature Communications*, 2020. https://doi.org/10.1038/s41467-020-17236-y.